JOURNAL OF MATERIALS SCIENCE **39** (2004) 1017– 1021

Discrete element modeling of solid formation during electrophoretic deposition

J. CORDELAIR, P. GREIL
Friedrich Alexander University of Erlangen – Nuremberg, Department of Materials Science (Glass and Ceramics), Martensstr. 5, 91058 Erlangen

Electrophoretic deposition (EPD) of colloidal ZrO_2 ceramic powder was examined with respect to the internal colloidal forces and the external electrical field. The influence of electrolytic dissociation of water close to the deposition electrode (cathode) on the electrostatic interaction between the particles and the local electric field is discussed. The discrete element method (DEM) was used to get an insight into the kinetics determining particle packing and density gradient microstructures. The simulation indicates that high particle concentrations combined with low electric field strength result in coagulated flocs and a low packing density in the deposit layer. Tentative phase diagrams for various colloidal forces and electrical field strengths were established.

1. Introduction

Ceramic manufacturing usually involves processing of inorganic powders into the desired component shape, followed by densification at elevated temperatures via solid or liquid state sintering. While conventional ceramics such as refractories, whitewares, tiles, etc. are manufactured from powder mixtures with one or more constituents having a particle size typically in the range above 10 μm, novel advanced materials such as high-strength engineering ceramics, thin solid electrolyte membranes, multilayer packages (MLCs), capacitors (MCCs), and actuators (MCAs), etc. require significantly smaller particle sizes in the colloidal size range, e.g., <1 μm. Colloidal powder processing offers the potential to reliably produce ceramic materials and products with improved microstructure homogeneity through careful control of particle to particle interaction in the initial suspension structure and its evolution during green body fabrication [1–3]. Although powder processing is a multibody problem prone to heterogeneities and nonuniform phase distribution, it is the most efficient method to form ceramics.

A distinct feature of colloidal ceramic suspensions is a large contact area between particles and the dispersing medium. Hence, interparticle (or surface) forces strongly influence suspension behavior and powder packing dynamics during shaping [4]. The various types of interparticle forces that govern suspension stability and rheology include van der Waals, electrostatic, steric and depletion forces. The kinetics and mechanics of powder consolidation into green bodies were analyzed for several forming routes, including pressure filtration [5, 6], slip casting [7], tape casting [8, 9], robocasting [10] and osmotic consolidation [11]. Scattering measurements have been an effective tool to study order-disorder [12], colloidal crystallization [13] and particle clustering transitions [14]. Furthermore, the many body nature of the colloidal interparticle interactions in concentrated suspensions is not well understood and there is a challenge for experimental and theoretical analysis of local suspension structure during consolidation.

Electrophoretic deposition (EPD) is a colloidal process wherein ceramic bodies are shaped directly from a colloidal suspension by the action of an electric field [15]. In a first step the charged particles (and ions) migrate towards the deposition electrode of opposite charge. In a second step the charged particles approach each other and coagulate at or near the surface of the deposition electrode forming a solid deposit layer. The principles of electrophoresis have been known since the last century, but different explanations to describe the mechanisms for depositing particles with some strength and internal cohesion can be found in literature [15]. It has been suggested that the primary function of the applied electric field is to accelerate the charged particles towards the electrode of opposite charge, the electrostatic coulomb force being the driving force. In case of low concentrated suspensions, the motion of the particles is determined by the equilibrium between electrical and frictional forces and a constant drift velocity can be found. When the solid load becomes higher close to the electrode surface, the individual particle mobility will be restricted and instead a collective (mechanical) pressure onto particles closer to the electrode surface is supposed to develop. The accumulated particles will be forced to flocculate and form a solid packing structure. Moreover, local flocculation near the electrode surface may be induced by electrolytic reactions which give rise for a distinct shift of the pH. Thus, if deposition in an aqueous suspensions occurs on a cathode, pH may be increased significantly

to the basic region, which may cause particles stabilized in acidic conditions to flocculate.

DEM has been developed in the late seventies [16] to simulate the flowing behavior of granular assemblies in civil engineering. Recently, it has been extended to model the movement of colloidal particles in ceramic suspensions [17]. In DEM each particle is treated as an individual element, each keeping its mass, radius and charge as a function of time and location, as well as parameters from local suspension properties such as ionic concentration, Debye parameter, pH and electric field strength. These data can be used to trace the movement of each powder particle in the suspension and thus allows to predict the particle packing behavior as derived from local suspension and particle properties.

The aim of this paper is to simulate the packing behavior during electrophoretic deposition of a submicron ZrO_2 powder from aqueous suspension. The ZrO_2 was positively charged and the deposition occurred on the cathode (cathaphoresis) under galvanostatic conditions (constant current load). DEM was used to calculate the packing structure under various stabilization conditions. Particular attention was paid to the electrolysis of water close to the electrode surface [18].

2. Experimental procedure

2.1. Powder system

A submicron ZrO_2 ceramic powder (Table I) was used to determine parameters for the simulation. The zeta potential was measured using the electrokinetic sonic amplitude technique (ESA 9800, Matec, Northborough, USA), where the sound wave was measured, when an alternating electric field was applied to the colloidal suspension. The zeta potential was calculated from the related dynamic mobility according to the model of O'Brien. It showed that the ZrO_2 powder had an isoelectric point of $pH_{iep} \approx 6.3$. At pH < 5 a high positive zeta potential of approximately 30–35 mV and at pH 8 a moderate negative zeta potential of –12 mV were found, Fig. 1.

Deposition on the negatively charged cathode was simulated starting from a suspension stabilized between pH 2.7–5.3 to achieve deposition from a stabilized suspension with the particles carrying a positive charge. Constant current conditions (galvanostatic) were assumed in order to simplify the numeric description for

TABLE I ZrO_2 powder characteristics

t-ZrO_2 powder		Suspension	
Mean particle size (nm)	840	Solvent	Water
Specific surface area (m^2/g)	7	Diffusion coefficient H^+ (10^{-5} cm^2/s)	9.31
Density (g/cm^3)	5.89	Viscosity (Pa s)	10^{-3}
Hamaker constant (10^{-20} J)	−7.23	Dielectric constant (ε_r)	78
Dielectric constant (ε_r)	18	Electrolyte concentrations (mmol/l)	0.02–3.5
Zeta potential at pH 4 (mV)	35		
Young's modulus (GPa)	205		
Poisson ratio	0.23		

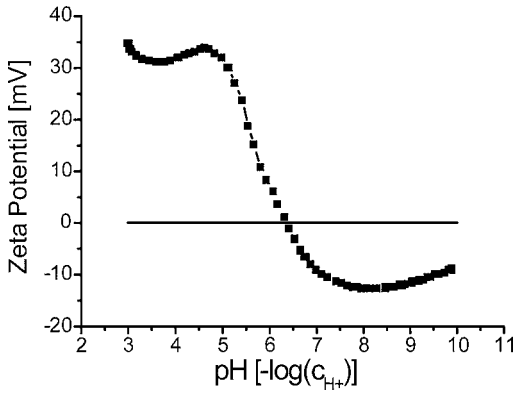

Figure 1 Zeta potential of ZrO_2.

the electrolytic dissociation of water at the electrode surface. The current density was varied from 0.2 to 1.6 mA/cm^2. When dispersing the suspension with Mg—stabilized ZrO_2-balls grinding balls, Mg^{++} and OH^- ions are inevitably released into the aqueous solution. Additionally the content of electrolytes in the aqueous ZrO_2 suspension was varied from 0.02 to 3.5 mmol/l $Mg(OH)_2$. Table I summarizes the simulation parameters used in the DEM calculations.

2.2. Discrete element method (DEM)

In DEM each particle is treated as an individual element. The motion of the particles in the suspension during processing (fluid flow) and forming (deposition) is calculated by using a discrete time stepping method. Newton's law of motion for particle i can be formulated according to

$$m\frac{\partial u_i}{\partial t} = \sum_j F_{ij} + f_i \qquad I\frac{\partial \omega_i}{\partial t} = \sum_j M_{ij} \quad (1)$$

where m and I are the mass and the moment of inertia of the particle, and u and ω are the directional and angular velocities, respectively [19]. The first term on the right hand side of these equations, F_{ij} and M_{ij}, are the sum of the force and moment resulting from the contact between the particles i and j. f_i is a non-colloidal force acting on the particle i which comprises frictional drag, rotational resistance, hydrodynamic lift, buoyancy, gravitation and migration in an electric field [17]. A numerical solution for Newton's law may be obtained using an explicit Euler time stepping scheme

$$(u_i)_{n+1/2} = (u_i)_{n-1/2} + \Delta t\frac{\sum_j F_{ij} + f_i}{m}$$
$$\omega_{n+1/2} = \omega_{n-1/2} + \Delta t\frac{\sum_j M_{ij}}{I}. \quad (2)$$

The corresponding position update equations are defined by

$$j_{n+1} = j_n + (u_j)_{n+1/2}\Delta t \quad \theta_{n+1} = \theta_n + \omega_{n+1/2}\Delta t. \quad (3)$$

At time $t + \Delta t$, these displacements are used to compute the new displacements at the end of the current time

increment. A single processor workstation (RISC/6000, IBM) equipped with 1 GB RAM was used to calculate the trajectories of a system of 300 particles. The results of the simulation were visualized with a series of snapshots that illustrate the transitional powder packing structure.

2.3. Particle interaction forces

The colloidal interaction between the particles suspended in a liquid medium, F_{coll} was derived by differentiation of the total interaction energy, V_{total}, by

$$F_{\text{coll}} = -\frac{\partial V_{\text{total}}}{\partial h} = -\frac{\partial (V_{\text{vdW}} + V_{\text{elec}})}{\partial h} \tag{4}$$

where h is the interparticle distance. The two energy terms constitute the well known DLVO model [20]. For the van der Waals interaction energy, V_{vdW}, the following expression was taken

$$V_{\text{vdW}} = -\frac{H}{6}\left[\frac{2a_1a_2}{h^2 + 2h(a_1 + a_2)} + \frac{2a_1a_2}{h^2 + 2h(a_1 + a_2) + 4a_1a_2} + \ln\left(\frac{h^2 + 2h(a_1 + a_2)}{h^2 + 2h(a_1 + a_2) + 4a_1a_2}\right)\right] \tag{5}$$

The Hamaker constant H for the system ZrO_2/H_2O was taken from literature ($H = 7.23 \times 10^{-20}$ J [2]). V_{elec} is the repulsive energy resulting from electrostatic interactions between like charged particle surfaces. It can be described for low ion concentrations with an electrostatic pair potential of the Yukawa type [21]

$$V_{\text{ij}}^{\text{el}} = \frac{Q_{\text{i}}^{\text{eff}} Q_{\text{j}}^{\text{eff}}}{\varepsilon(h + a_{\text{i}} + a_{\text{j}})} \exp[-\kappa(h + a_{\text{i}} + a_{\text{j}})] = \frac{Q^{\text{eff}2}}{\varepsilon(h + a_{\text{i}} + a_{\text{j}})} \exp[-\kappa(h + a_{\text{i}} + a_{\text{j}})]. \tag{6}$$

ε is the dielectric constant of the solvent ($\varepsilon = 78\varepsilon_0$ for water) and Q^{eff} the charge of equal particles. The effective charge of particle i, $Q_{\text{i}}^{\text{eff}}$, is related to the colloidal charge

$$Q_{\text{i}} = a\varepsilon(1 + \kappa a)\Psi_0$$

via

$$Q_{\text{i}}^{\text{eff}} = \frac{Q_{\text{i}} \exp[\kappa a]}{1 + \kappa a} \tag{7}$$

where Ψ_0 is the zeta potential [21]. The Debye–Hückel parameter κ depends mainly on the ion concentration and is defined by [20]

$$\kappa = \sqrt{\frac{e_0^2 \sum c_{\text{i}} z_{\text{i}}^2}{\varepsilon k T}}. \tag{8}$$

For the system under consideration $1/\kappa$ was estimated to vary in the range from 38 to 2.7 nm.

3. Results

3.1. Electrolysis of water

Hydrogen and oxygen are generated during current load at the cathode and anode, respectively, according to the overall reaction equation

$$\begin{aligned} &2H_2O_{(1)} + 2e^- \Rightarrow 2H_{2(g)} + 2OH^- \quad \text{Cathode reaction} \\ &2H_2O_{(1)} \Rightarrow O_{2(g)} + 4H^+ + 4e^- \quad \text{Anode reaction} \end{aligned} \tag{9}$$

The reduction to H_2 is associated with the flow of 2 electrons and the formation of $2OH^-$ ions at the cathode surface which gives rise for an OH^- concentration profile depending on the distance to the electrode surface and on time. When migration is neglected, the motion of OH^- ions is dominated by diffusion and can be described by Fick's law

$$\frac{\partial c_{\text{OH}^-}}{\partial t} = D_{\text{OH}^-} \frac{\partial^2 c_{\text{OH}^-}}{\partial^2 x} \tag{10}$$

where c_{OH^-} is the concentration and D_{OH^-} the diffusion coefficient of OH^-. Under galvanostatic conditions (constant current density j) the time dependence of the OH^- concentration c_{OH^-} at the electrode surface can be described by

$$c_{\text{OH}^-}(t)|_{\text{x=0}} = c_0 + \frac{2mj}{nF\sqrt{\pi D}}\sqrt{t} \tag{11}$$

where F is the Faraday constant m the multiplicity of a single reaction step and n the electrode reactivity ($m = 2$, $n = 2$ for the cathode reaction) [22]. With increasing current load time the concentration profile extends more and more into the suspension, raising the OH^- concentration near to the cathode. A reasonable approximation for the dependence of the concentration profile $c_{\text{OH}^-}(x, t)$ on the distance to the electrode surface, x, can be formulated with respect to the Nernst diffusion layer thickness δ_{N}

$$\delta_{\text{N}} = \frac{n}{m} FD \frac{c_{\text{OH}^-}(t)|_{\text{x=0}} - c_0}{j} \tag{12}$$

$$c_{\text{OH}^-}(x, t) = \left(1 - \frac{x}{\delta_{\text{N}}}\right)(c_{\text{OH}^-}(t)|_{\text{x=0}} - c_0) + c_0. \tag{13}$$

For $x > \delta_{\text{N}}$ the OH^- concentration is given by the equilibrium concentration c_0. Charge neutrality in the system under consideration requires that the concentration of cations is equal to the concentration of anions

$$c_{\text{H}^+} + 2c_{\text{Mg}^{++}} = c_{\text{OH}^-}. \tag{12}$$

Taking into account the law of mass action for the electrolyte—water system as

$$c_{\text{H}^+}(x, t) \cdot c_{\text{OH}^-}(x, t) = c_{\text{H}^+}(x, 0) \cdot (c_{\text{H}^+}(x, 0) + 2c_{\text{Mg}^{++}}) = K \tag{13}$$

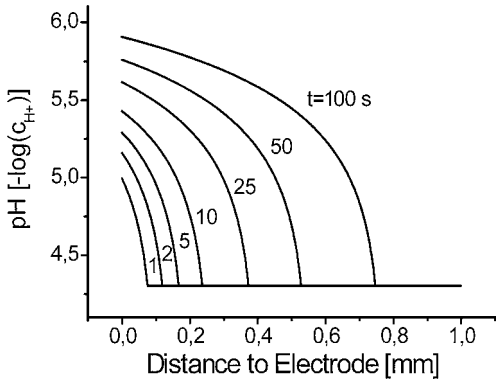

Figure 2 pH close to the cathode deposition electrode as a function of surface distance and time (pH 4.3, $j = 0.2$ mA/cm^2, $Mg(OH)_2 = 0.02$ mmol/l).

where K is the dissociation constant of the solution, the development of the pH close to the cathode surface could be estimated as a function of time (t), distance to electrode surface (x) and current density (j) (Fig. 2) [23], and the charge and zeta potential of the particles is also time and location dependent in the Nernst layer. The release of ions from the particles due to the change of pH is very small (for a pH 4 suspension with particle concentration of 1 vol% the particle charge is below 10^{-10} mol/l) and is not considered in the simulation.

3.2. DEM-simulation of particle deposition

While in the as prepared suspension the particles are uniformly distributed, distinct differences in particle distribution structures can be observed during deposition. With increasing solid concentration homogeneous nucleation of flocs occur in a zone between the solid deposit and the colloidal suspension. Depending on pH, electrolyte—concentration, current—density and mass—flow, the particles in the zone close to the deposit layer mutually repell (stable state), weakly attract (flocculated state) or strongly attract (coagulated state) each other, Fig. 3. In the stable state the particles form a highly ordered deposit with a maximum packing density on the electrode, Fig 3a. The transition from the suspension to the solid is characterized by a sharp boundary (growing deposit surface). Formation of regions where the particles are weakly bound to each other (in a secondary minimum of the interaction energy function) characterizes the flocculated state, Fig. 3b. These aggregates accumulate at the electrode forming a non-uniform packing structure where domains of high order are interconnected. If the suspension was initially set to the flocculated state the size of the aggregates depends mainly on the age of the suspension. The aggregation process of coagulated colloid clusters can be best viewed as diffusion limited aggregation (DLA [24]), Fig. 3c. Depending on solid load, large deeply fissured clusters are generated. These clusters accumulate at the electrode into a loose colloid network. The two dimensional packing density in the three different areas attains 51.6% from a coagulated, 65.8% from a flocculated and 80.3% from a stable suspension, respectively. The maximum possible packing density of 90.7% (hexagonal closed packing) of monomodal spheres in two dimensions is not achieved due to the incorporation of packing defects.

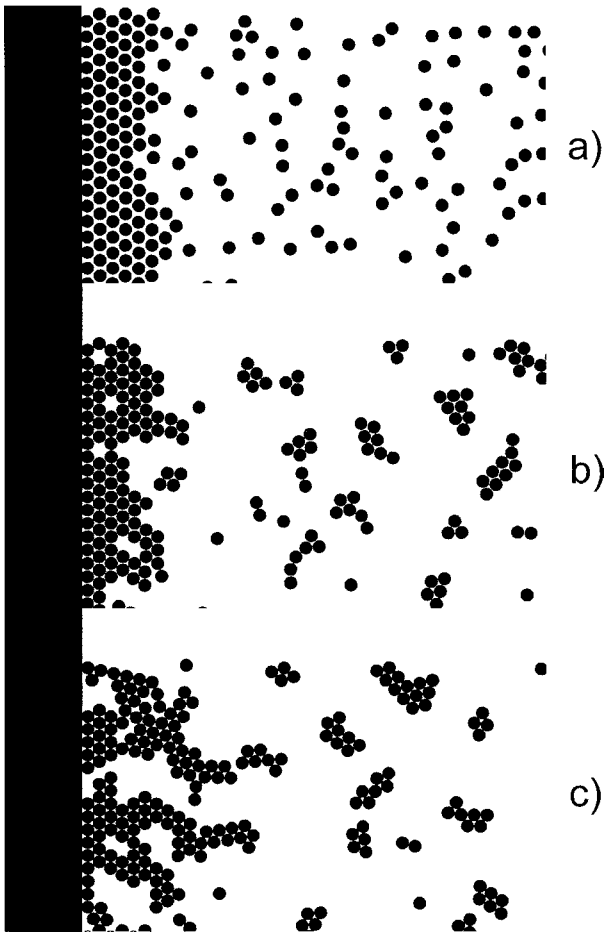

Figure 3 Particle distribution structures in the Nernst layer: (a) stable state, (b) flocculated state, and (c) coagulated state.

4. Discussion

Fig. 4 shows tentative phase diagrams constructed from the simulation data. Fig. 4a presents a phase diagram depending on the electrolyte concentration and particle area fraction in the Nernst layer of a suspension at pH 4 after 2 s with a current load of 0.2 mA/cm^2. The phases were classified according to the scheme used in Fig. 3 where circles indicate the stable, triangles the flocculated and rectangles the coagulated state. Additionally the color indicates when the coagulated state is reached: black symbols are for a coagulation transition time $t_c < 10$ s, gray, $t_c < 30$ s and white, $t_c > 30$. The phase diagram shows that only for low electrolyte concentrations (>0.1 mmol/l) the stable state can be observed. With increasing electrolyte concentration the depth of the secondary minimum gets deeper, thus particles are effectively bound to each other, when they come close enough. For electrolyte concentrations exceeding 2.7 mmol/l the suspension falls into the coagulated state. Fig. 4b shows the simulated phase diagram depending on initial pH and particle area fraction in the Nernst layer of a suspension after 2 s with a current load of 0.2 mA/cm^2. At pH < 3 the suspension is in the flocculated state. Between 3 and 4.5 the suspension is in the stable state offering best deposition conditions. Above pH 4.5 a low current result in large pH variations

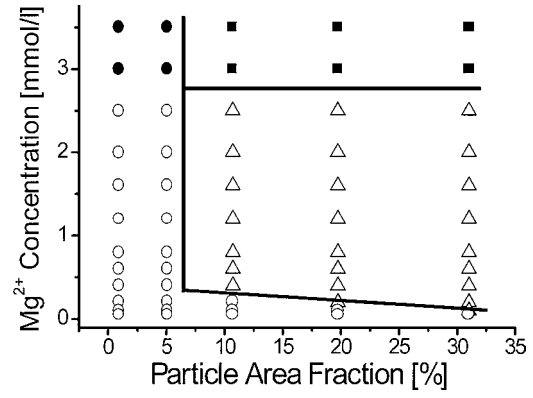

(a)

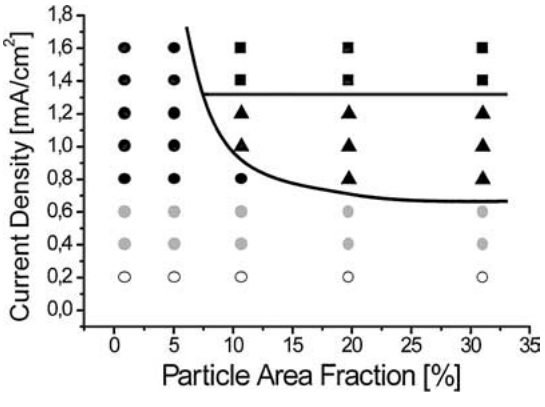

(b)

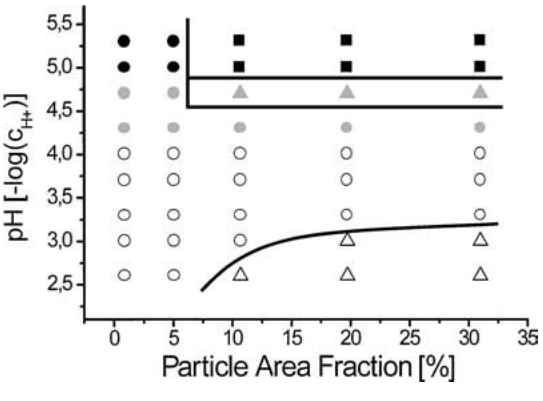

(c)

Figure 4 Tentative phase diagrams of the transition zone ahead of the growing deposit (Nernst layer): (a) Effect of electrolyte concentration, (b) Effect of current density, and (c) Effect of initial pH.

thus the suspension in the transitional ordering zone comes quickly into the coagulated state.

Fig. 4c shows the simulated phase diagram depending on current density and particle area fraction in the Nernst layer of a suspension at pH 4 without electrolyte after 2 s current load. At current densities below 0.4 mA/cm^2 the suspension is in the stable state but it would last very long if ever to coagulate the particles at the electrode to form the deposit. Between 0.4 and 0.8 mA/cm^2 the suspension is still in the stable state but t_c fell below 30 s thus deposition may take place when no convection is present. At current densities above 0.8 mA/cm^2 the suspension is in the flocculated state and t_c is below 10 s. Current densities above 1.3 mA/cm^2 result in fast coagulation in the Nernst layer.

5. Conclusions

DEM simulation of the electrophoretic deposition of ZrO_2 powders indicated the formation of flocculated and coagulated particles in the Nernst layer ahead of the growing solid deposit. A novel approach to EPD presented in this paper by smooth phase transitions shows a strategy to avoid these problems by smart control about process parameters. Tentative phase diagrams have been derived from the packing structure simulations to evaluate the influence of the particle area fraction, current density, electrolyte concentration and initial pH. They can be used to select improved processing parameters for achieving highly dense and uniformly packed sediments by electrophoretic deposition techniques.

Acknowledgement

Financial support from Deutsche Forschungsgemeinschaft (DFG) under Grant No. HO 1670/7 is gratefully acknowledged.

References

1. F. F. LANGE, *J. Amer. Ceram. Soc.* **72** (1989) 3.
2. J. A. LEWIS, *ibid.* **83** (2000) 2341.
3. W. M. SIGMUND, N. S. BELL and L. BERGRSTRÖM, *ibid.* **83** (2000) 1557.
4. J. C. CROCKER and D. G. GRIER, *MRS Bull.* (1998) 24.
5. D. S. ADCOCK and I. C. McDOWELL, *J. Amer. Ceram. Soc.* **40** (1957) 355.
6. T. J. FENNELLY and J. S. REED, *ibid.* **55** (1972) 264.
7. R. R. ROWLAND, *Amer. Ceram. Soc. Bull.* **45** (1966) 16.
8. R. E. MISTLER, *ibid.* **69** (1990) 1022.
9. R. PITCHUMANI and V. M. KARBHARI, *J. Amer. Ceram. Soc.* **78** (1995) 2497.
10. J. CESERANO, R. SEGALMAN and P. CALVERT, *Ceram. Industry* **94** (1998) 94.
11. K. T. MILLER and C. F. ZUKOSKI, *J. Amer. Ceram. Soc.* **77** (1994) 2473.
12. R. L. HOFMAN, *Trans. Soc. Rheol.* **16** (1972) 155.
13. A. VAN BLAADEREN, R. RUEL and P. WILTZIUS, *Nature (London)* **385** (1997) 321.
14. J. BENDER and N. J. WAGNER, *J. Rheol.* **16** (1972) 155.
15. P. SARKAR and P. S. NICHOLSON, *J. Amer. Ceram. Soc.* **79** (1996) 1987.
16. P. A. CUNDALL and O. D. L. STRACK, *Géotechnique* **29** (1979) 47.
17. C. W. HONG, *J. Amer. Ceram. Soc.* **80** (1997) 2517.
18. P. GREIL, J. CORDELAIR and A. BEZOLD, *Z. Metallkunde* **92** (2001) 682.
19. K. ODA, T. SHIGEMATSU and T. ONISHI, in Proc. 2nd Int. Conf. On Discrete Element Methods (DEM) (IESL Publ., MIT, Cambridge (MA), 1993) p. 165.
20. E. J. W. VERWEY and J. TH. G. OVERBEEK, "Theory of Stability of Lyophobic Colloid" (Elsevier, Amsterdam, 1948).
21. H. LÖWEN and G. KRAMPOSTHUBER, *Europhys. Lett.* **23** (1993) 673.
22. C. H. HAMANN and W. VIELSTICH, "Elektrochemie" (Wiley-VCH, Weinheim, 1998).
23. D. DE and P. S. NICHOLSON, *J. Amer. Ceram. Soc.* **82** (1999) 3031.
24. A. K. ARORA and B. V. R. TATA, "Ordering and Phase Transitions in Charged Colloids" (VCH-Wiley, Weinheim, Germany, 1996).

Received 18 June 2002
and accepted 16 September 2003